18th International Conference on Information Fusion
Washington, DC - July 6-9, 2015

Non-Line-of-Sight Mitigation for Reliable Urban GNSS Vehicle Localization Using a Particle Filter

Sven Bauer, Robin Streiter and Gerd Wanielik
Technische Universität Chemnitz
Email: firstname.lastname@etit.tu-chemnitz.de

Marcus Obst
Baselabs GmbH
Email: marcus.obst@baselabs.de

***Abstract*—GNSS based localization in the context of Advanced Driver Assistance Systems and autonomous driving raises its attention regarding positioning performance not only related to accuracy but integrity as well. Especially, for safety relevant applications the proper computation of confidence levels under degraded environmental conditions is of major importance. Low cost solutions that integrate GNSS and additional in-vehicle sensor information are able to bridge short periods of time with limited GNSS accessibility and can therefore improve availability and accuracy. Additionally, non-line-of-sight (NLOS) and multipath effects in urban areas need special attention as these error influences violate the estimated confidence and introduce unobservable offsets to the position solution. The mitigation of local influences in urban areas increases the demands for the integration of proper error models for NLOS and multipath errors. The algorithmic detection of these effects and the proper propagation of all uncertainties within a Bayes framework is one of the key technologies towards the adoption of GNSS for safety critical applications. This paper proposes a probabilistic NLOS detection algorithm that is able to improve both - accuracy and integrity of the position estimate in urban areas. As an extension of a previous implementation by the authors based on an unscented Kalman Filter the proposed system is implemented as a particle filter in order to meet automotive requirements in terms of real time and scalability. Both approaches are compared by an evaluation of a data set from an urban test drive in terms of accuracy and integrity.**

I. Introduction

Reliably knowing the precise position of the ego vehicle is required for a large number of advanced driver assistance systems (ADASs). Low-cost off-the-shelf GPS receivers are getting integrated into most standard commercial vehicles making satellite-based localization one of the most promising candidates for this task. Although these GNSS receivers deliver a suitable performance under good geometric constellations and free signal reception conditions that offers street level precision for low-demanding applications this cannot always be guaranteed. However, besides the accuracy of the position solution, this guaranteed reliability and availability are two key aspects for many intelligent transportation systems (ITSs). More challenging conditions like signal blockage or disturbed signal reception cause the positioning performance to degrade. This can often be observed in dense urban environments where close buildings or the foliage of an avenue cause those non-line-of-sight (NLOS) or multipath effects. Detecting and handling blocked signals is hereby the easier task, this can be directly observed as the expected GNSS measurements are not available anymore. Reliably doing so for reflected and otherwise disturbed GNSS signals is more difficult. The measurements are still available, but using them during the localization process leads on one hand to an unmodelled bias in the resulting position estimate and to the violation of the then underestimated confidence interval of the positioning solution. As those effects are a rapidly changing phenomenon in an urban environment it is hard to detect and predict it[1].

Given those limitations for classical GNSS-only localization, it can be summarized that reliable positioning is still a challenging task. For ITS applications like tolling, green driving assistants for efficient path planning and even upcoming safety applications like intersection assistants a reliable positioning is required, showing that further work on this area is still needed. The aim of this paper is to propose a generic online GNSS positioning algorithm for vehicular applications with integrated probabilistic NLOS mitigation using a particle filter. The algorithm can be used to autonomously increase localization accuracy and integrity without additional hardware sensors. Even if the algorithm is not restricted to urban areas, its biggest impact can be expected in strong multipath-affected situations.

The paper is structured as follows: In the first section, an overview of related work and state-of-the-art technologies for GNSS localization and NLOS mitigation is given. Afterwards, the fundamentals of satellite navigation and Bayesian filtering are briefly introduced. The next section contains a description of the probabilistic NLOS mitigation and its proposed adaption to a particle filter. In the following section, the implementation of the presented system is given. In the subsequent section the generated results are presented and discussed. The paper concludes with a summary and an outlook of future research.

II. Related Work

An overview of so called Multipath Mitigation algorithms is given in [2]. A straightforward approach is identifying multipath by considering digital maps with modeled 3D buildings in order to validate the direct line-of-sight (LOS) to each satellite. In the Bayesian framework this approach is used to predict multipath affected GNSS observations [3]. Another algorithm for determining NLOS with the help of environmental knowledge is described in [4][5]. A NLOS signal detection respecting the satellite shadows in an urban scenario is presented in [6].

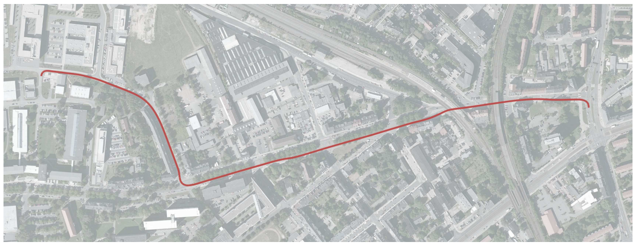

Fig. 1. Overview of the used test track. Starting at the left with initially free line-of-sight conditions the reception conditions get worse. Especially the left turn under heave non-line-of-sight conditions and the two railway underbridges are challenging for GNSS only solutions.

Another group is based on additional hardware like a multi-antenna approach in [7] for checking the consistency of the GNSS signal reception. An infrared camera to identify NLOS measurements is proposed in [8]. A similar approach using a laser scanner to create a 3D model of the surroundings from point cloud data was shown in [9]. As these approaches cause additional costs to implement and do not rigorously implement the Bayesian framework (which is assumed to be required for safety relevant applications) the next group is of significant interest.

This group uses statistic tests and probabilistic filtering for the identification and mitigation of multipath. A known representative in this category is Receiver Autonomous Integrity Monitoring algorithm (RAIM) and its extensions [10]. However, classical RAIM is limited to handle a single outlier within the measurement set, it is therefore not fully appropriate for urban multipath situations as proven in [11]. This limitation is not shared by a fully probabilistic alternative given in [12]. In [13] an approach based on robust pose graph optimization for offline processing for multipath mitigation is introduced.

III. Fundamentals

A. Satellite Navigation

The core working principle of GNSS positioning is based on simultaneously measuring the distance between the receiver antenna and multiple satellites at one epoch. To compute a position from those measurements usually four unknowns need to be resolved:

$$x_{\text{receiver}} = \begin{pmatrix} x & y & z & dt \end{pmatrix}^{\mathrm{T}} \tag{1}$$

Three unknowns belong to the three dimensional position coordinate on earth and an additional one is required to account for the clock bias dt of the GNSS receiver relative to the GNSS system time. Therefore, to process this using a standard least-squares estimator, at least four ranging measurements are required. As those time of flight observations are impaired by multiple additional error sources they are often called pseudoranges and modeled[14] as:

$$\rho = r + c(dt - dT) + d_{\text{ion}} + d_{\text{trop}} + d_{\text{eph}} \tag{2}$$

In the given equation, ρ denotes the observed pseudorange and r the true geometric distance between the receiver and the satellite. The other terms account for various error sources that disturb this relation. In this example $c(dt - dT)$ denotes the ranging error duo to the satellite clock error dT and the user clock error dt relative to the common GNSS time base; with the speed of light c. Furthermore, the signal is subject to propagation delays caused along its signal path through the ionosphere d_{ion} and through the troposphere d_{trop}. For the receivers position calculation the satellites position must also be known. Those are usually computed from the broadcasted ephemerides, which are only accurate to around one meter and represent by the last error term d_{eph}.

B. Non-Line-of-Sight Error

Other errors are not accounted for by this model, which will normally lead to a bias in the final position estimate. Most of them have a negligible influence on the positioning performance, like the measurement noise of the receiver which translates to an additional noise of the final position. However, this is not the case for non-line-of-sight effects which can frequently be observed in an urban setting. In such an environment corrupted NLOS measurements - also often called multipath - can typically disturb the measured pseudorange length by up to 150 m and therefore significantly impair the systems performance. To cope with this problem an additional error term d_{mul} can be introduced into (2):

$$\rho = r + c(dt - dT) + d_{\text{ion}} + d_{\text{trop}} + d_{\text{eph}} + d_{\text{mul}} \tag{3}$$

However, in contrast to the slowly changing global effects like the ionospheric or tropospheric delay, modeling d_{mul} is an extremely challenging task. It heavily depends on the local environment around the receiver and changes rapidly as the receiver is moved through it.

C. Particle Filter

The particle filter belongs to the group of sequential Monte Carlo methods. In contrast to a Kalman filter the probability density function (PDF) of a system's n_x-dimensional state vector $x_k \in \mathbb{R}^{n_x}$ is not described in a parametric way like a Gaussian but uses statistically drawn samples instead to approximate the PDF. These samples can then be transformed even using non-linear functions and thereby overcome a Kalman filters limitations like the requirement of a Gaussian PDF, linear state transition and observation functions or a continuous state space.

A simple particle filter is the implementation of the often called Sampling-Importance-Resampling (SIR) schema, which is the combination of sequential importance sampling with an importance resampling. The first allows the recursive state estimation update only requiring a state transition function and its likelihood as well as the previous sample weights. However, this algorithm suffers from a degeneracy problem which causes most samples weights to get close to zero leaving only a few samples with a representative weight impairing their probability density representation. The importance resampling counters this problem by creating equally weighted particles from weighted ones. To achieve this, samples with a low or close to zero weight are deleted while samples with high weights are duplicated[15].

IV. Probabilistic Non-Line-of-Sight Detection

Instead of such an explicit modeling of the NLOS error, the authors previously introduced concept of a probabilistic multipath detection and mitigation in [12] and [16] for use in an Unscented Kalman Filter (UKF) is adapted and applied to a particle filter.

The main idea of the algorithm is similar to generalized probabilistic data association (GPDA) used in vehicle tracking. The GNSS receivers' pseudorange measurements $z^1, \ldots, z^{n_z}$ make up the measurement set $\{z\}$. This set is divided into the two subsets $\{z\}^{\text{valid}}$ and $\{z\}^{\text{invalid}}$ which contains the valid and the invalid NLOS affected measurements, respectively.

However, this assignment is not known a priori. To solve this, the algorithm defines the set of all possible association hypotheses. From a probabilistic point of view, these hypothesiss represent discrete association events $A_j^m \in A^m \subset A$. The subsets A^m contain all association events A_i^m which are based on the assumption that exactly m measurements are received under LOS conditions. The cardinality of A^m is given by $\binom{n_z}{m}$, where n_z denotes the cardinality of $\{z\}$. Therefore, the maximum number of assumed LOS measurements is given by n_z and the minimum number is zero.

The complete set of association events is given by

$$A = \begin{cases} A^0 & = \begin{cases} A_0^0 & \text{if } \{z\} = \{z\}^{\text{NLOS}} \end{cases} \\ A^1 & = \begin{cases} A_1^1 & \text{if } z^1 \text{ is LOS} \\ \vdots & \\ A_{n_z}^1 & \text{if } z^{n_z} \text{ is LOS} \end{cases} \\ A^2 & = \begin{cases} A_1^2 & \text{if } z^1 \text{ and } z^2 \text{ are LOS} \\ A_2^2 & \text{if } z^1 \text{ and } z^3 \text{ are LOS} \\ \vdots & \end{cases} \\ \vdots & \\ A^{n_z} & = \begin{cases} A_1^{n_z} & \text{if } \{z\} = \{z\}^{\text{LOS}} \end{cases} \end{cases} \tag{4}$$

Although integrating this into an UKF with the goal to condition the posterior state PDF on the association events showed a significant improvement of the positioning performance[16], several drawbacks of it are addressed by this papers approach:

- The performance heavily depends on the number of visible satellites.
- At every time step all hypothesis are evaluated.
- Problematic weight normalization between hypothesiss with a different number of valid measurements.

As the UKF implementation needs to test and asses each hypothesis, the algorithms run time depends exponentially on the number of observed GNSS satellites giving a time complexity of $O(2^{n_z})$. At the moment, a GPS only system usually observes around 7 satellites at a time with a possible maximum of 12. However, more and more GNSS receivers are nowadays multi-constellation enabled. Besides the American GPS, they also process the signals of other satellite systems like the Russian GLONASS, the Chinese BeiDou or the upcoming European Galileo which increasing the number of visible satellites considerably. This would require a pruning strategy to maintain an except-able performance for such an algorithm. In contrast, the proposed particle filter uses a constant number of particles to estimate the system state yielding a stable run time. For this papers evaluation 5000 particles are used, although preliminary tests indicated that around 1000 to 2000 seemed to be sufficient. This suggest a break-even point of ca. 11 observed satellites.

This is enabled by making the binary LOS/NLOS state of each satellite part of the systems state space, estimating it over time. The assumption that those flags are short-time constant also models the real world expectation better and allows the exploitation of the temporal coherence of the NLOS effect. Although this effect quite rapidly changes, it is usually caused by the local environment the vehicle passes through. For example, a satellites signal is freely received until the vehicle passes a nearby building which obscures the signal path and causes the NLOS state while passing it.

Another problem of the previous implementation lies in the computation of the weights the filter needs to assign to each hypothesis. This is computed as the product of the so called validity and spatial likelihood. The former expresses how likely a LOS/NLOS hypothesis appears to be while the last expresses the likelihood that the hypothesis produces the observed measurements. For this, the valid LOS measurements are used to evaluate an m-variate Gaussian obtained from the Kalman filters predicted PDF of the pseudoranges. However, as we are unable to predict NLOS measurements, a uniform distribution with a adjustable gate width was used instead. Although sound, further analysis showed that this exponential term mainly adjusts for the different magnitudes the m-variate Gaussian evaluates to. Its biggest effect is on the null hypothesis that assumes all measurements are unusable NLOS measurements, balancing it to the other hypothesiss.

V. Implementation

A. Vehicular Motion Model

To model the vehicles motion a Constant Turn Rate and Velocity (CTRV) model as described in [17] was chosen. The system state space of this model can be described as

$$^{\text{CTRV}}x = \begin{pmatrix} x & y & \theta & \omega & v \end{pmatrix}^{\text{T}} \tag{5}$$

where x, y and z describe the position of the vehicle within a cartesian coordinate system (e.g. UTM). θ represents the heading direction the vehicle is driving into, ω its change rate (the yaw-rate) and v the vehicles velocity. The CTRV models state transition equation is

$$x_{k+1} = \begin{pmatrix} x_k + \frac{1}{\omega_k}(v_k(sin(\omega_k T + \theta_k) - sin(\theta_k))) \\ y_k + \frac{1}{\omega_k}(v_k(-cos(\omega_k T + \theta_k) + cos(\theta_k))) \\ \theta_k + \omega_k T \\ \omega_k \\ v_k \end{pmatrix}. \quad (6)$$

It describes how the system state evolves from one time step k to $k+1$ where $T = t_{k+1} - t_k$ is the time span between both steps.

B. GNSS Tightly Coupling

Instead of computing a position solution using the GNSS receivers pseudorange measurements and using this as the input for the positioning filter a so called tightly coupling is used. With this approach the pseudorange observations are directly used as the input for the filter which has two advantages:

1) No information loss or reduction at the least squares stage.
2) It allows for a position update with less than four satellite measurements.

To allow this, the particle filter must be able to predict pseudorange measurements for a given system state space in order to update the weight of the samples by comparing them to the real observations. From equation 2 is clear that the true geometric distance r is required. For a satellite i at time step k this is given by

$$r_k^i = \sqrt{(x_k^i - x_k)^2 + (y_k^i - y_k)^2 + (z_k^i - z_k)^2}. \quad (7)$$

The ith satellites position (x_k^i, y_k^i, z_k^i) for the time step can be obtained from the broadcasted ephemerides. However, the CTRV system state space needs to be expanded from its two dimensional receiver position to three dimensions. Furthermore, the receivers' clock bias dt is necessary to predict the clock error term; the satellites clock error dT can again be computed from the broadcasted ephemerides. In addition, to improve the modeling of the receiver clock its clock drift dt_{drift} relative to the GNSS time is included too. The GPSs Klobuchar model [18] used to model the ionospheric delay d_{ion} and the Saastamoinen model used to model the tropospheric delay d_{trop} do not require any additional data and d_{eph} is neglected. To integrate the probabilistic NLOS mitigation into the filter, a binary flag identifying the assumed LOS or NLOS state is added to the space as well. Thus, the fully extended CTRV system state space ${}^{\text{CTRV,GNSS}}x$ to directly process pseudorange observations is defined by

$${}^{\text{CTRV,GNSS}}x = \begin{pmatrix} x & y & z & \theta & \omega & v & v_z & dt & dt_{\text{drift}} & \text{los}^{0 \ldots n_i} \end{pmatrix}^{\text{T}}. \quad (8)$$

As required by this change, the state transition equation 6 has been adopted to

$$x_{k+1} = \begin{pmatrix} x_k + \frac{1}{\omega_k}(v_k(sin(\omega_k T + \theta_k) - sin(\theta_k))) \\ y_k + \frac{1}{\omega_k}(v_k(-cos(\omega_k T + \theta_k) + cos(\theta_k))) \\ z_k + v_{z_k} T \\ \theta_k + \omega_k T \\ \omega_k \\ v_k \\ v_{z_k} \\ dt_k + dt_{\text{drift}_k} T \\ dt_{\text{drift}_k} \\ \text{los}_k^{1 \ldots n_z} \end{pmatrix} \quad (9)$$

which models the receivers altitude z with a constant climb rate v_z, its clock bias dt with a constant clock drift dt_{drift} and the line-of-sight classification of each satellite as constant.

C. Empirical Sensor Model

Although the proposed algorithm can work without additional knowledge for the LOS/NLOS distribution, incorporating such is possible and further benefits its precision. Instead of fusing information of additional costly sensors into the positioning filter, a byproduct of the GNSS receiver itself is incorporated. The used u-blox LEA4T GNSS receiver, like most GNSS receivers, also outputs the information about the signal-to-noise ratio (SNR) of its satellite measurements.

In the authors previous work [12] an empirical likelihood model for LOS and NLOS assessment is derived. To create the free LOS model the same low-cost GPS receiver as used for the later evaluation was installed at a fixed roof mounted position which ensured free LOS visibility. The pseudoranges, the SNR values as well as the satellite elevation angles were collected during a continuous long-term measurement campaign of nine days in Chemnitz, Germany with an update rate of 1 Hz. As can be expected, the SNR values depend on the satellites elevation angle. Therefore, the empirical statistical properties assuming a normal distribution are calculated for each discrete elevation angle in the range of $0°$ to $90°$ separately. With this knowledge, the free LOS likelihood $p(\text{SNR} = s|\text{LOS})$ can be calculated by evaluating the normal distribution corresponding to the measurements elevation angle for a given SNR observation.

In contrast to the given previous work, to create a likelihood model for $p(\text{SNR} = s|\text{NLOS})$ several hours of various recorded test drives of the professorship have been evaluated. Hereby it was exploited that the test vehicles centimeter level reference ground truth system consisting of a Novatel SPAN system with RTK and IMU support omits largely inconsistent satellite observations. In addition, the ground truth systems pseudorange measurements were compared to the expected pseudorange measurement for the given receiver position and the satellite position computed using precise SP3 orbit products[19]. The u-blox measurements of times where the ground truth omitted a satellites measurements or the difference between the ground truth measurement and the expectation exceeded a threshold of 20 m were then used to derive the NLOS model. The satellites elevation again proved to be a key influence, but as a normal distribution was a bad match to the classified SNR measurements a uniform distribution was chosen instead to reflect the relative low information content.

D. Particle Filter

The implementation of the particle filter follows the schema described in section III-C. At each measurement epoch, which usually contains several pseudorange observations, the following steps are performed:

1) Filter pseudorange observations.
2) Perform low variance resampling.
3) Predict particle states.
4) Update particle probabilities.

At the first step all observations that are deemed unusable are removed from the observation set. This is only the case for observations whose satellite position cannot be computed yet due to insufficient received ephemeris data and for satellites below the elevation mask angle of $15°$.

In the following step the low variance resampling – adopted from [15] – is performed to prevent the weight degradation keeping the particles a good representation of the estimated system state probability density.

At step three the state transition function is applied to each particle predicting its state to the measurement epoch. In table I the standard deviation of the used process noise parameters is given. While applying the additive zero-mean noise is straight forward for most state space values, special care must be taken of the LOS flag due to its binary nature. A new hypothesis combination of the LOS flags is uniformly drawn from all available possible permutations if one of the following conditions is met:

- A previously observed satellite is not available anymore.
- A new satellite is observed.
- The value drawn from the uniform distribution $\mathcal{U}(0,1)$ is less than the process hypothesis noise parameter σ_{hyp}.

The first two conditions ensure that obsolete information is discarded and that each available satellite is classified. The third is a tuning parameter that adjusts how constant the expected line-of-sight conditions are expected to be. At the extreme case of $\sigma_{\text{hyp}} = 0\,\%$ the system model assumes that the LOS conditions are truly constant and never change while $\sigma_{\text{hyp}} = 100\,\%$ assumes this to be extremely volatile so that the entire particle mass is used to constantly test all LOS/NLOS hypothesis.

The final step is the sequential importance samplings update of each particles probability weight. For this, each samples probability weight is multiplied by its new states likelihood $P_{k+1,m}$, where m identifies the sample. This is the combination of two likelihoods, the validity likelihood and spatial likelihood. The validity likelihood defines the probability that the samples LOS/NLOS hypothesis is correct, if such an assessment is possible. At this paper, the empirical sensor model described in section V-C is used. The validity likelihood of satellite i is hereby

TABLE I
PROCESS NOISE PARAMETERS USED BY THE CTRV MODEL BASED FILTERS

Parameter	TC	UKF	Particle
Acceleration	18.95 m/s^2	5.12 m/s^2	15.08 m/s^2
Altitude acceleration	2.49 m/s^2	5.91 m/s^2	2.40 m/s^2
Angular acceleration	2.50 rad/s	2.56 rad/s	2.24 rad/s
Clock drift acceleration	18.36 m/s^2	59.77 m/s^2	8.53 m/s^2
Gate Width	-	4.01	-
Hypothesis Noise	-	-	45,39 %

TABLE II
PARAMETERS FOR THE EMPIRICALLY DERIVED RESIDUAL DISTRIBUTIONS.

Parameter	Value
LOS normal distribution - μ	0.67 m
LOS normal distribution - σ^2	5.11 m^2
NLOS Laplace distribution - μ	0.52 m
NLOS Laplace distribution - b	9.60 m

$$P(z^i_{\text{snr}}|x^i_{\text{los,m}}, z^i_{\text{el}}) = \begin{cases} f_{\text{los}}(z^i_{\text{snr}}, z^i_{\text{el}}) & \text{if } x^i_{\text{los,m}} \text{ is true} \\ f_{\text{nlos}}(z^i_{\text{snr}}, z^i_{\text{el}}) & \text{if } x^i_{\text{los,m}} \text{ is false} \end{cases} \tag{10}$$

where f_{los} evaluates the LOS models normal distribution and f_{nlos} the NLOS models uniform distribution for the satellites elevation angle z^i_{el} at the measured SNR z^i_{snr}. As the local conditions are unknown the satellites validity likelihoods are assumed to be independent giving the samples overall validity likelihood as

$$P_{\text{m,validity}} = \prod_{j=1}^{n_z} P(z^j_{\text{snr}}|x^j_{\text{los,m}}, z^j_{\text{el}}). \tag{11}$$

To assess the spatial likelihood the difference between the measured pseudorange and the predicted pseudorange is used to evaluate empirical residual distributions that have been created alongside the SNR sensor model using the same data but without the elevation based separation (see section V-C). For the LOS case a normal distribution has been fitted while the NLOS residuals follow a Laplace distribution. Their parameters are listed in table II. This yields, equivalent to equations 10 and 11,

$$P(z^i_{\rho}|x^i_{\text{los,m}}) = \begin{cases} f_{\text{los}}(z^i_{\rho}) & \text{if } x^i_{\text{los,m}} \text{ is true} \\ f_{\text{nlos}}(z^i_{\rho}) & \text{if } x^i_{\text{los,m}} \text{ is false} \end{cases} \tag{12}$$

$$P_{\text{m,spatial}} = \prod_{j=1}^{n_z} P(z^j_{\rho}|x^j_{\text{los,m}}) \tag{13}$$

and updates the *m*th particles weight ω_m to

$$\omega_{m,k+1} = \omega_{m,k} * P_{\text{m,validity}} * P_{\text{m,spatial}}. \tag{14}$$

TABLE III
ACCURACY AND PERCENTAGE OF FIXES WITHIN THE ESTIMATED CONFIDENCE INTERVAL

Algorithm	RMSE	$\overline{3\sigma}$	σ	2σ	3σ
Least Squares	8.4 m	14.7 m	66.4 %	92.1 %	97.2 %
Tightly Coupled	7.7 m	7.9 m	16.7 %	68.8 %	80.4 %
UKF	5.3 m	12.5 m	42.1 %	98.8 %	100.0 %
Particle	4.6 m	8.9 m	32.8 %	88.8 %	96.2 %

VI. RESULTS

To evaluate the particle filters NLOS mitigation its positioning performance is compared to the results of a weighted least squares (LS) solver as described in [14], a tightly-coupled Bayes Filter (TC) and the Unscented Kalman Filter implementation of the NLOS mitigation (UKF). For the evaluation raw GNSS sensor observations from an ublox LEA-4T low-cost single frequency GPS receiver are used. They were recorded during an urban test drive within the city of Chemnitz which includes NLOS conditions at straight sections and during turns as well as two railway underbridges, see figure 1. The data collection has been done with the prototyping vehicle CARAI [20] which is available at Chemnitz University of Technology. It is also equipped with a high-reliable reference GNSS system that provides a ground truth trajectory with centimeter-level accuracy. The particle filter was configured to use 5000 samples which a preliminary test indicated to be overly sufficient. To select the process noise parameters shown in table I for each of the three filter candidates a maximum likelihood optimization using the Covariance Matrix Adaption Evolution Strategy [21] was performed so that each filter produced the most plausible solution. For each of the four algorithms, the horizontal position error in relation to the ground truth and the corresponding confidence interval was calculated. Furthermore, for the position errors the root mean square error (RMSE) for the whole sequence is calculated as well. For a reliable positioning algorithm, the number of solutions outside the estimated confidence interval should be rather small. For example, taking the $3\,\sigma$ measure yields that 99.7% of all possible solutions shall be within the estimated interval. For the sake of completeness, the average of the estimated confidence interval denoted by $3\,\sigma$ is calculate as well.

In table III the resulting RMSE and the average estimated 3σ integrity interval for all four algorithms is given. As expected, the weighted least squares and the simple tightly coupled filter perform worst under such difficult conditions. Non-line-of-sight effects are not modelled which causes several large position errors. As both algorithms are unaware of this the estimated confidence intervals remain quite static. For the least squares approach they directly depend upon the number of observed satellites and their slowly changing geometric constellation while the tightly coupled filter adds some noise-like dynamic to it, this can be seen in figure 2 and 3. The pseudorage measurement accuracy estimation of the least squares algorithm, that is used to weight the

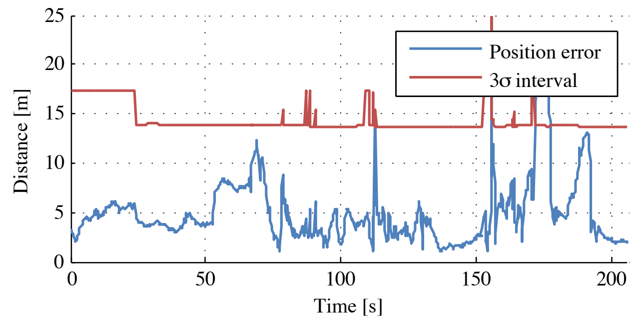

Fig. 2. Estimation results for weighted least squares solution. The almost static confidence interval is only subject to the number of observed satellites and their geometric constellation.

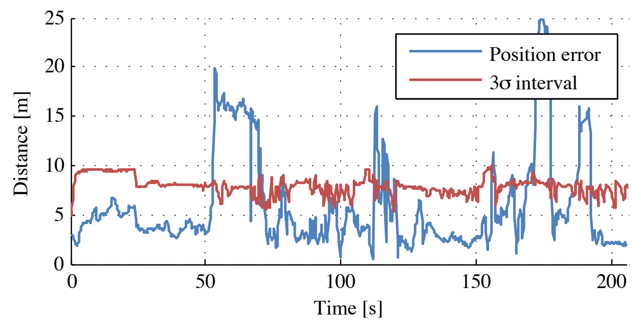

Fig. 3. Estimation results for tightly coupled Bayes filter. As NLOS conditions are not considered they cause outliers well above the relatively even 3σ interval.

measurements, is based upon the elevation and correction models. These cause, in contrast to the distributions used for the other algorithms, a relative high integrity interval estimation. This helps in mitigating the first NLOS sequence after second 50 but yields the largest integrity interval reducing the dependability of its solution. However, a non-weighted least squares produce larger errors and a much smaller 3σ estimation further worsening the result.

The solution of the UKF-based NLOS mitigation is shown in figure 4. In comparison to the tightly coupled filter the RMSE is reduced by 31 % to 5.3 m and the integrity estimation now adapts to the environmental challenged receiving conditions. Although this raises the average interval estimation by almost 60 %, making it almost as large as the least squares estimate, comparing figure 3 and 4 indicates that this is mainly caused by the increased estimation during assumed NLOS sequences. This also meets the expectations from a theoretical point of view. As both filters use the same basic measurement and motion models the integrity estimation during free LOS conditions should be comparable while the down weighting of NLOS hypotheses and thereby the less relying at the measured pseudoranges increases the estimation.

The particle filter based approach is visualized in 5. It achieves a further reduction of the RMSE by 13 % to 4.6 m. In comparison to the UKF-based implementation a very similar

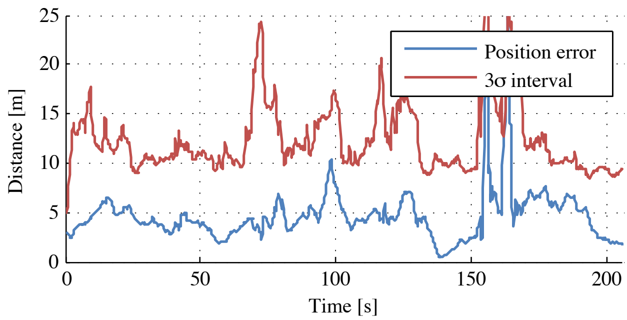

Fig. 4. Estimation results for the UKF based NLOS mitigation implementation. A large confidence interval that reflects the local circumstances is estimated and large outliers are mitigated.

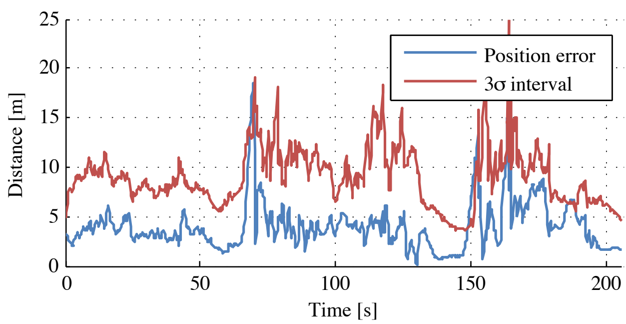

Fig. 5. Estimation results for the Particle Filter based NLOS mitigation implementation. The position error got reduced further, but the shrunk confidence interval is violating it more often now.

behavior can be observed although the estimated confidence interval is significantly reduced too. As a result, the position estimates more often violates the 1 to 3 σ interval. One possible explanation for this behavior is the number of satellites used by both algorithms. For this, the normalized weighted sum of the number of satellites within the LOS hypothesises of both algorithms is shown in figure 6. Although it can be seen that the particle filter tends to rely more on particles with more LOS classified satellites than the UKF implementation does - especially for free LOS sequences, this ratio is almost balanced at difficult NLOS areas. This matches the observed lower confidence estimation at the begin of the test sequence, however a higher increase during bad receiving conditions would have been expected.

VII. Conclusion

Within this paper, an algorithm for GNSS-based vehicular positioning based on a particle filter and empirical data was proposed and evaluated. Therein the focus was set on the mitigation of non-line-of-sight effects like multipath that are most challenging within an urban area. The paper at hand addresses problems of an earlier but already promising probabilistic approach by using a particle filter that now could incorporate a more suitable constant LOS/NLOS model. This was implemented and validated using real world measurements

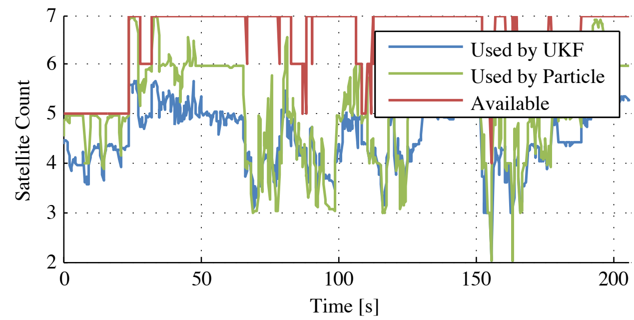

Fig. 6. Comparison of the statistical number of effectively used satellites. Under free LOS conditions the particle filter considers more satellites useable which reduces its confidence estimation.

of an urban test drive. Using this scenario it was shown that the new approach further reduced the positioning error by 13 % or 0.7 m. The confidence interval estimated alongside of the vehicle state was reduced as well. However, this lead to more position samples exceeding it, a possible disadvantage for applications that need to rely on it. As the algorithm is intended for online processing in a vehicle, it is real-time capable on current PC hardware and could be further optimized due to the parallel nature of a particle filter.

Besides a deeper analysis of the integrity short-coming, further research will include the integration of odometry/INS sensor that is available in nowadays vehicles, the integration of GNSS Doppler measurements for GNSS only applications as well as a deeper analysis of the algorithms application to multi-constellation GNSS positioning.

Acknowledgment

For the evaluation and generation of the ground truth, precise real-time corrections provided by ascos (http://www.ascos.de) were used.

References

[1] G. Duchateau, O. Nouvel, W. Vigneau, D. Betaille, F. Peyret, and H. Secretan, "How to assess and improve satellite positioning performances in urban environments," in *16th ITS World Congress, Stockholm, 2009: Proceedings*, 2009.

[2] P. D. Groves, Z. Jiang, M. Rudi, and P. Strode, "A portfolio approach to nlos and multipath mitigation in dense urban areas," *Proceedings of the 26th International Technical Meeting of The Satellite Division of the Institute of Navigation*, 2013.

[3] M. Obst, S. Bauer, P. Reisdorf, and G. Wanielik, "Multipath detection with 3d digital maps for robust multi-constellation gnss/ins vehicle localization in urban areas," in *Proceedings of the IEEE Intelligent Vehicles Symposium*, 2012.

[4] F. Peyret, D. Betaille, P. Carolina, R. Toledo-Moreo, A. Gomez-Skarmeta, and M. Ortiz, "Gnss autonomous localization: Nlos satellite detection based on 3-d maps," *Robotics Automation Magazine, IEEE*, vol. 21, no. 1, pp. 57–63, March 2014.

[5] C. Pinana-Diaz, R. Toledo-Moreo, D. Betaille, and A. Gomez-Skarmeta, "Gps multipath detection and exclusion with elevation-enhanced maps," in *Intelligent Transportation Systems (ITSC), 2011 14th International IEEE Conference on*, Oct 2011, pp. 19–24.

[6] P. Groves, Z. Jiang, L. Wang, and M. Ziebart, "Intelligent urban positioning, shadow matching and non-line-of-sight signal detection," in *Satellite Navigation Technologies and European Workshop on GNSS Signals and Signal Processing, (NAVITEC), 2012 6th ESA Workshop on*, Dec 2012, pp. 1–8.

[7] D. Egea, G. Seco-Granados, and J. Lopez-Salcedo, “Single- and mwulti-correlator sequential tests for signal integrity in multi-antenna gnss receivers,” in *Localization and GNSS (ICL-GNSS), 2014 International Conference on*, June 2014, pp. 1–6.

[8] J. Meguro, T. Murata, J. Takiguchi, Y. Amano, and T. Hashizume, “Gps multipath mitigation for urban area using omnidirectional infrared camera,” *Intelligent Transportation Systems, IEEE Transactions on*, vol. 10, no. 1, pp. 22–30, March 2009.

[9] T. Suzuki and N. Kubo, “Gnss multipath and diffraction mitigation using 3d digital surface model in urban canyon,” in *Proceedings of the 24th International Technical Meeting of The Satellite Division of the Institute of Navigation (ION GNSS 2012)*, 2012.

[10] Z. Qiang, Z. Xiaolin, and C. Xiaoming, “Research on raim algorithm under the assumption of simultaneous multiple satellites failure,” in *Software Engineering, Artificial Intelligence, Networking, and Parallel/Distributed Computing, 2007. SNPD 2007. Eighth ACIS International Conference on*, vol. 1, July 2007, pp. 719–724.

[11] O. L. Marchand, P. Bonnifait, J. Banez-Guzman, F. Peyret, and D. Betaille, “Performance evaluation of fault detection algorithms as applied to automotive localisation,” in *European Navigation Conference GNSS 2008*, 2008.

[12] M. Obst and G. Wanielik, “Probabilistic Non-Line-of-Sight Detection in Reliable Urban GNSS Vehicle Localization based on an Empirical Sensor Model,” in *Intelligent Vehicles Symposium (IV), 2013 IEEE*, 2013.

[13] N. Sünderhauf, M. Obst, G. Wanielik, and P. Protzel, “Multipath mitigation in gnss-based localization using robust optimization,” in *Intelligent Vehicles Symposium (IV), 2012 IEEE*, June 2012, pp. 784–789.

[14] E. Kaplan and C. Hegarty, *Understanding GPS: principles and applications*. Artech House Publishers, 2006.

[15] S. Thrun, W. Burgard, and D. Fox, *Probabilistic robotics*, ser. Intelligent robotics and autonomous agents. MIT Press, Sep. 2005.

[16] M. Obst, S. Bauer, and G. Wanielik, “Urban multipath detection and mitigation with dynamic 3d maps for reliable land vehicle localization,” in *IEEE/ION PLANS*, 2012.

[17] R. Schubert, C. Adam, M. Obst, N. Mattern, V. Leonhardt, and G. Wanielik, “Empirical evaluation of vehicular models for ego motion estimation,” in *Proceedings of the IEEE Intelligent Vehicles Symposium*, 2011, accepted for publication.

[18] J. Klobuchar, “Ionospheric time-delay algorithm for single-frequency gps users,” *Aerospace and Electronic Systems, IEEE Transactions on*, vol. AES-23, no. 3, pp. 325–331, May 1987.

[19] J. Dow, R. Neilan, and C. Rizos, “The international gnss service in a changing landscape of global navigation satellite systems,” in *Journal of Geodesy*, vol. 83, 2009, pp. 191–198.

[20] R. Schubert, E. Richter, N. Mattern, P. Lindner, and G. Wanielik, *Advanced microsystems for automotive applications 2010 : smart systems for green cars and safe mobility*. Springer, 2010, ch. A Concept Vehicle for Rapid Prototyping Of Advanced Driver Assistance Systems, pp. 211–219.

[21] N. Hansen, “The CMA evolution strategy: a comparing review,” in *Towards a new evolutionary computation. Advances on estimation of distribution algorithms*, J. Lozano, P. Larranaga, I. Inza, and E. Bengoetxea, Eds. Springer, 2006, pp. 75–102.